Observation of Mrk421 during 2008 with ARGO-YBJ

S. Vernetto*, D. Martello‡, J.L. Zhang¶, on behalf of the ARGO-YBJ Collaboration

**IFSI-INAF and INFN, Torino, Italy*
‡*Dip. di Fisica dell'Università del Salento and INFN, Lecce, Italy*
¶*Institute of High Energy Physics, Chinese Academy of Science, Beijing, P.R. China*

***Abstract*. The ARGO-YBJ experiment, a full coverage air shower detector located at Yangbajing (4300 m asl, Tibet, China) monitored Mrk421 during the whole 2008, at gamma ray energies E $>$ 0.8 TeV. The observed signal was variable, with the strongest flares in March-June, in good correlation with X-rays measurements. The average emission during the interval from day 41 to day 180 was about twice the Crab Nebula level, with an integral flux of 4.9$\pm 2.0 \times 10^{-11}$ photons cm^{-2} s^{-1} for energy E $>$ 1 TeV, and decreased afterwards.**

This paper concentrates on the flares occurred in the first half of June. This period has been studied from optical to 100 MeV gamma rays, and only partially up to TeV energies, since the moonlight hampered the Cerenkov telescope observations during the second and most intense part of the emission. Our data complete these observations, with the detection of a signal of intensity of about 7 Crab units on June 11-13, with a statistical significance of 4.2 standard deviations. The observed flux is consistent with a prediction made in the framework of the Synchrotron Self-Compton model, in which the flare is caused by a rapid acceleration of leptons in the jet.

***Keywords*: gamma ray sources, blazar, air showers**

I. Introduction

The blazar Mrk421 is known for its strong flaring activity on times scales ranging from minutes to months. Strong correlation between gamma rays and X-rays has been reported during many active periods [1], [2]. This correlation can be interpreted in terms of the Synchrotron Self-Compton model (SSC) in which X-rays photons are attributed to synchrotron radiation from high energy electrons accelerated in the jet, while VHE photons are due to inverse Compton scattering of the same electrons off the synchrotron photons [3]. This mechanism produces a spectral energy distribution (SED) characterized by a double-hump structure with a first peak usually in the soft to medium X-ray range, and a second one at GeV - TeV energies [4], [5]. The simultaneous observation at different wavelengths can provide unique information about the source properties and the radiation processes.

A set of simultaneous measurements covering 12 decades of energy, from optical to TeV gamma rays, was performed during the strong flaring activity on the first half of June 2008 by different detectors: WEBT (optical R-band), UVOT (UV), RXTE/ASM (soft X-rays), SWIFT (soft and hard X-rays), AGILE (hard X-rays and gamma rays) and the Cherenkov telescopes VERITAS and MAGIC (VHE gamma rays). [6].

In this period two flaring episodes were reported, the first one on June 3-8, observed from optical to TeV gamma rays, the second one, larger and harder, on June 9-15, observed from optical to 100 MeV gamma rays. Using the multi frequency data, Donnarumma et al. derived the SED for June 6, that shows the typical two humps shape, in agreement with the SSC model. According to the authors, the second hump intensity (that reached a flux of about 3.5 Crab units at energy E $>$400 GeV) seems to indicate that the variability is due to the hardening/softening of the electron spectrum, and not to the increase/decrease of the electron density. Their model predicts for the second flare a VHE flux about a factor 2 larger with respect to the first one. Unfortunately there were no VHE data included in their multi-wavelength analysis after June 8 because the moonlight hampered the Cherenkov telescopes measurements. The VHE observation was actually done for such a very important flaring episode by the ARGO-YBJ experiment, that since 2007 December has been performing a continuous monitoring of Mrk421.

II. The ARGO-YBJ experiment

The ARGO-YBJ experiment, located at the Yangbajing Cosmic Ray Laboratory (Tibet, P.R. China, 4300 m a.s.l., 30° 06' 38" N, 90° 31' 50" E), is constituted by a central carpet $\sim$74$\times$78 m^2, made of a single layer of Resistive Plate Chambers (RPCs) with $\sim$93% of active area, enclosed by a guard ring with partial coverage, which allows to extend the instrumented area up to $\sim$100$\times$110 m^2. The apparatus has a modular structure, the basic data acquisition element being a cluster (5.7$\times$7.6 m^2), each made of 12 RPCs (2.8$\times$1.25 m^2). Each chamber is read by 80 strips of 6.75$\times$61.8 cm^2 (the spatial pixel), logically organized in 10 independent pads of 55.6$\times$61.8 cm^2 which are individually acquired and represent the time pixel of the detector. The full detector is composed of 153 clusters for a total active surface of $\sim$6600 m^2 [7].

Operated in *shower mode*, ARGO-YBJ records all events with a number of fired pads $N_{pad} \geq 20$ in the central carpet in a time window of 420 ns. The spatial coordinates and the time of any fired pad are then used to reconstruct the position of the shower core and the arrival direction of the primary [8].

Since November 2007 the detector is in stable data taking with a trigger rate of ~3.6 KHz.

III. Detector performance

The angular resolution and the pointing accuracy of the detector have been evaluated by using the Moon shadow, i.e. the deficit of cosmic rays in the Moon direction. The shape of the shadow provides a measurement of the detector Point Spread Function (PSF), and its position allows to find out possible pointing biases. ARGO-YBJ observes the Moon shadow with a sensitivity of about 10 standard deviations per month for events with a multiplicity $N_{pad} \geq 40$ and zenith angle $\theta <50°$, corresponding to a proton median energy $E_p \sim 1.8$ TeV.

According to the Moon shadow data, the PSF of the detector is Gaussian for $N_{pad} \geq 100$, while for lower multiplicities it can be described with an additional Gaussian, which contributes for about 20%. When the PSF is a Gaussian with r.m.s. σ, the opening angle ψ containing ~71.5% of the events maximizes the signal to background ratio for a point source with a uniform background, and it is equal to 1.58 σ.

The semi aperture ψ is 2.59°± 0.16°, 1.30°± 0.14 and 1.04°± 0.12° respectively for $N_{pad} \geq 40$, 100 and 300, in agreement with expectations from Monte Carlo simulations[9].

This measured angular resolution refers to cosmic rays-induced air showers. The angular resolution for γ-induced events has been evaluated by simulations and it is 10-30% smaller (depending on N_{pad}), due to the better defined time profile of the showers.

IV. Data Analysis

The dataset for the analysis of Mrk421 presented in this paper contains all showers with $N_{pad} \geq 40$ and zenith angle less than 40°.

A 20°×20° sky map in celestial coordinates (right ascension and declination) with 0.1°×0.1° bin size, centered on the source location, is filled with the detected events. In order to extract the excess of γ-ray coming from the source, the cosmic rays background must be carefully estimated and subtracted from the event map. The background is evaluated with the *time swapping* method [10]. For each detected event, N "fake" events are generated by replacing the original arrival time with new ones, randomly selected from a buffer that spans about 3 hours of data taking. Changing the time, the "fake" events maintain the same declination of the original event, but have a different right ascension. With these events a new sky map (background map) is built.

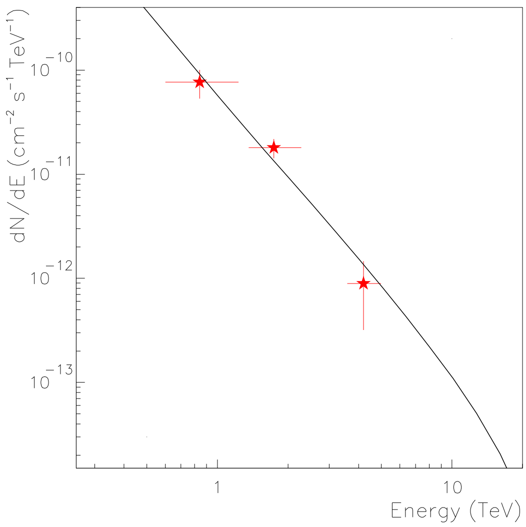

Fig. 1: Differential energy spectrum of Mrk421 obtained by ARGO-YBJ from 2008 day 41 to 180, when the source was in active state. The line represents the best fit to the data.

By using 10 fake events per real event, the statistical error on the background can be kept sufficiently small.

The two maps are then "integrated" over a circular area of radius ψ, i.e. every bin is filled with the content of all bins whose center has an angular distance less than ψ from its center, where ψ is the radius of the window containing 71.5% of the signal, i.e. ψ = 1.9°, 0.9° and 0.5° respectively for $N_{pad} \geq 40$, 100 and 300.

The next step is the correction of the background for the non uniformity of the cosmic ray flux [11] producing regions of excesses and deficits that can alter the significance of the sources. The adopted correction procedure is given in [12].

Finally the integrated background map is subtracted from the corresponding integrated event map, obtaining the "source map", where for every bin the statistical significance of the excess is calculated.

This analysis procedure has been tested with the Crab Nebula, the standard candle for VHE astronomy. The obtained energy spectrum is in agreement with other experiments[13].

The same analysis has been performed for Mrk421. This source culminates at the ARGO-YBJ location at a zenith angle $\theta_{culm} = 8.1°$, and it is observable every day for 6.38 hours with a zenith angle $\theta < 40°$.

ARGO-YBJ observed Mrk421 from 2007 day 311 to 2008 day 366. The gamma ray flux was variable in time, with the largest flares in March-June 2008.

Using the same method adopted for the Crab Nebula, we evaluated the Mrk421 spectrum from 2008 day 41 to day 180, where the X-ray flux showed the most intense flares. In this period (755 observation hours) the observed signal had a statistical significance of 6.1 standard deviations.

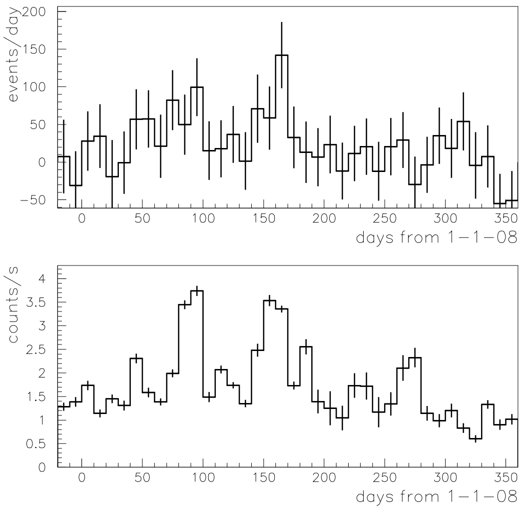

Fig. 2: Upper panel: excess event rate detected by ARGO-YBJ with N_{pad} ≥100, as a function of time, averaged over 10 days. Lower panel: X-ray counting rate detected by RXTE/ASM, averaged over 10 days.

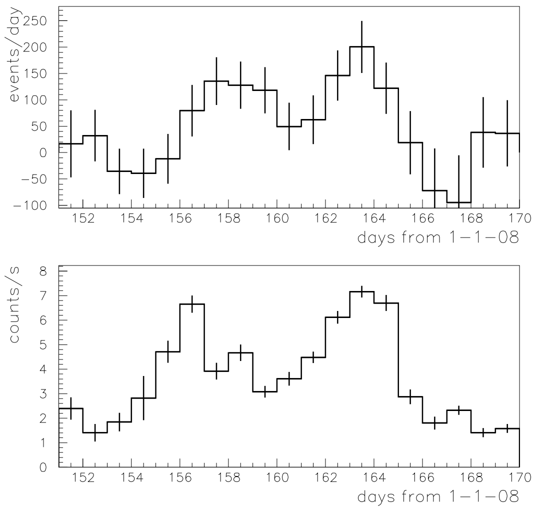

Fig. 3: Upper panel: rate of events with N_{pad} ≥100 (after event selection) observed by ARGO-YBJ as a function of time from May 31 00:00 UT to June 19 00:00 UT. Each bin contains the rate averaged over the 3 days interval centered on that bin. Lower panel: daily counting rate of RXTE/ASM.

We assumed a power law spectrum K $\times E^{\alpha}$ multiplied by an exponential factor $e^{-\tau(E)}$ to take into account the absorption of gamma rays on the Extragalactic Background Light (EBL), where the values of $\tau(E)$ are given by [14]. Then we simulated a source in the sky following the diurnal path of Mrk421, and evaluated the number of events expected in the 3 N_{pad} bins: 40-99, 100-299 and ≥300, for different values of K and α ($10^{-11} <$ K $< 10^{-10}$ and $1.5 < \alpha < 3.5$). Comparing the expected values with the observed ones we obtained the spectrum that best fits to data: dN/dE = (7.46±1.70) $\times$ $10^{-11}E^{-2.51\pm0.29}$ $e^{-\tau(E)}$ photons cm^{-2} s^{-1} TeV^{-1} (see Fig.1).

The integral flux above 1 TeV is 4.9±2.0 $\times$ 10^{-11} photons cm^{-2} s^{-1}, about twice the Crab Nebula flux. The median energies corresponding to the 3 N_{pad} bins previously described are respectively: E = $0.84^{+0.39}_{-0.24}$, $1.74^{+0.54}_{-0.38}$ and $4.2^{+0.79}_{-0.62}$ TeV.

The observed gamma ray rate appears to be correlated with the X-ray rate measured by the All Sky Monitor detector aboard the RXTE satellite in the 1.5-12 KeV energy range, as expected from the SSC model. Fig. 2 shows the rate of the excess events with N_{pad} ≥100 observed by ARGO-YBJ as a function of time, averaged over 10 days, compared to the corresponding X-rays counting rate of RXTE/ASM[15].

Now we focus our analysis on the VHE emission during the June 2008 flares studied by Donnarumma et al. As reported in the introduction, two different flares have been observed, the first one peaking in X-rays on June 5-7, the second one on June 12-13. Concerning VHE gamma rays, Cherenkov telescopes data are available only for the first flare. An energy spectrum for E ≥400 GeV has been provided by VERITAS for June 6.

Since the ARGO-YBJ sensitivity doesn't allow to observe a flux of few Crab units in only one day (i.e. during one transit of the source in the detector field of view), we integrated the measurement over 3 days.

Fig. 3 shows the rate of events with N_{pad} ≥100 observed by ARGO-YBJ during the first half of June, averaged over 3 days, compared with the X-ray flux measured by RXTE/ASM[15]. The source has been detected with a statistical significance of 3.2 standard deviations during the interval 11-13 June, when the maximum of the second flare occurred. The significance increases to 4.2 standard deviations rejecting the events with the core position at a distance larger than 60 m from the detector center, and with the χ^2 values given by the reconstruction fitting procedure larger than a suitable threshold, for which the arrival direction has been determined with less accuracy.

Fig. 4 shows the $6^{\circ}\times6^{\circ}$ sky map around the source position in these 3 days, after applying the event selection. For every $0.1^{\circ}\times0.1^{\circ}$ bin, the map gives the value of the statistical significance of the excess of events inside the circular window of radius 0.9° centered on that bin.

Donnarumma et al. evaluate a theoretical SED curve for the first flare fitting the observations made on June 6 from optical up to VHE energies. During the second flare, they reported a higher photon flux from soft X-rays to 100 MeV gamma rays. From these data they predict a flux at E $>$ 1 TeV of 1.45 $\times$ 10^{-10} photons cm^{-2} s^{-1} corresponding to about 7 Crab units, and they model a SED curve with the Inverse Compton hump slightly shifted towards higher energies.

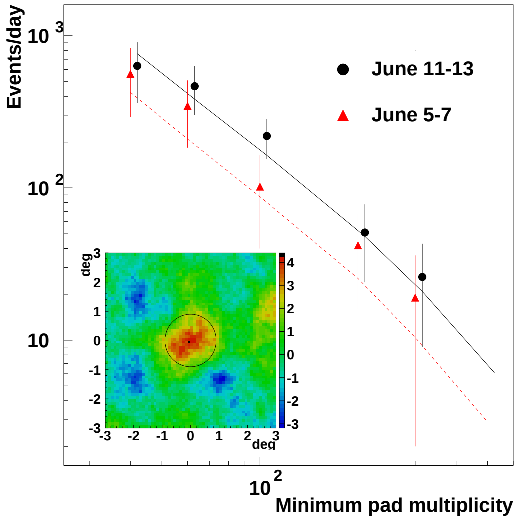

Fig. 4: Event rates observed by ARGO-YBJ as a function of the event minimum pad multiplicity on June 5-7 and June 11-13 (respectively red triangles and black circles). Expected rates according to the Donnarumma et al. model for the same two periods (respectively red dashed and solid black lines). The inset represents the sky map around the Mrk421 position on June 11-13, obtained for events with $N_{pad} \geq 100$. The colour scale on the right represents the significance of the signal in standard deviations. The circle represents the observational window of radius 0.9°

Fig. 4 shows the event rate observed by ARGO-YBJ (in 18.2 hours of measurement) compared with the rate expected from a source spectrum given by the theoretical SED, for any N_{pad} interval. The agreement is good.

A similar analysis is made for the first flare, integrating our data on June 5-7 (17.9 hours of measurement). The observed signal has a significance of $\sim$ 2 standard deviations, increased to 3.0 using the data selection. The event rate obtained as a function of the minimum pad multiplicity, is consistent with the one predicted by the SED of Donnarumma et al. for June 6 (see Fig.4).

Finally we estimate the energy spectrum for the second flare (the low significance of the first flare doesn't allow the spectrum evaluation). Following the same method described previously, we divided the events into 3 pad multiplicity bins: 40-99, 100-299 and $\geq$300. Assuming a source spectrum given by the theoretical SED, the median energy of the events in the 3 bins are respectively 0.9, 1.4 and 2.4 TeV.

Fig.5 gives the measured SED for the 3 energy points, together with all the measurements in the optical-TeV range, and the theoretical SED for the two flares.

The measurements appear in fair agreement with the expected emission.

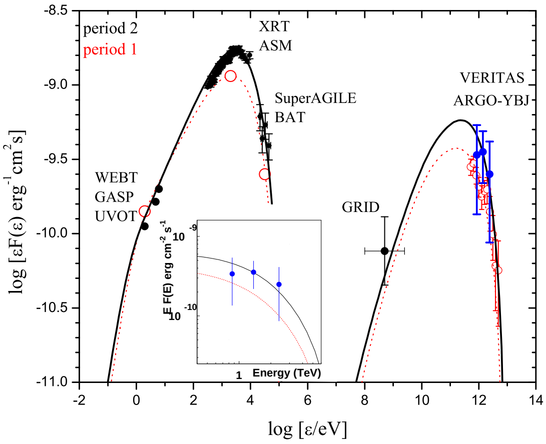

Fig. 5: Spectral energy distribution measured by ARGO-YBJ on June 11-13 (large blue filled circles) together with the data of other experiments, obtained during the first flare (red open circles), and the second one (black filled circles). The curves represent the SEDs modeled by Donnarumma et al. for the first flare (red dashed line) and the second one (black solid line). The inset shows a zoom on the ARGO-YBJ data.

V. Conclusions

In summary, Mrk421 has been continuously monitored with ARGO-YBJ during 2008, showing a VHE flux twice the Crab Nebula level from day 41 to 180, and decreasing afterwards.

Two strong flares in June 2008 has been observed in a multiwavelength campaign from optical to TeV energies. ARGO-YBJ measured the spectra of Mrk421 above 0.8 TeV during the second flare completing the multifrequency observations. For the first time an air shower array was able to detect gamma-ray flaring activity at sub-TeV energies on a few days period.

References

[1] Fossati G., Buckley J.H., Bond I.H. et al., 2008, ApJ, 677, 906
[2] Wagner R.M., 2008, PoS(BLAZARS2008), 63, 013 (arXiv:0809.2843)
[3] Ghisellini G., Celotti A., Fossati G. et al., 1998, MNRAS, 301, 451
[4] Sambruna R. M., Maraschi L. and Urry, C., 1996, ApJ, 463, 444
[5] Fossati G., Maraschi L., Celotti A. et al., 1998, MNRAS, 299, 433
[6] Donnarumma I. et al., 2008, ApJ, 691, L13
[7] Aielli G. et al., 2006, NIM A562, 92
[8] Di Sciascio G. et al., 2007, Proc. 30th ICRC, Merida, Mexico (arXiv:0710.1945)
[9] Di Sciascio G. et al., 2009, Proc. 31th ICRC, Lodz, Poland
[10] Alexandreas D.E. et al., 1992, NIM A311, 350
[11] Abdo A.A. et al, 2008, Phys.Rev.Lett. 101, 221101
[12] Vernetto S. et al, 2009, Proc. 31th ICRC, Lodz, Poland
[13] Marsella G. et al, 2009, Proc. 31th ICRC, Lodz, Poland
[14] Primack J.R., Bullock, J.S. and Sommerville R.S., 2005, AIP Conference Proceedings, 745, 23
[15] RXTE/ASM public data http://xte.mit.edu/asmlc/ASM.html